Anti fungal property of nanosized ZnS particles synthesised by sonochemical precipitation

P. Suyana[a], S. Nishanth Kumar[b], B. S. Dileep Kumar[b], Balagopal N. Nair[c], Suresh C. Pillai[d], A. Peer Mohamed[a], K. G. K. Warrier[a] and U. S. Hareesh[a]*

[a]Material Science and Technology Division

[b]Agroprocessing and Natural Products Division

National Institute for Interdisciplinary Science and Technology (CSIR-NIIST)

Thiruvananthapuram-695019, India

[c]R& D Centre, Noritake Co. Limited, Aichi 470-0293, Japan

[d] Department of Environmental Science, Institute of Technology Sligo, Ash Lane, Sligo,

Ireland

*Corresponding author E-mail: hareesh@niist.res.in

Telephone: 0091 4712535504   Fax: 0091 471 2491712

Abstract

Zinc Sulphide (ZnS) nanoparticles, synthesised by sono-chemical route employing zinc chloride and sodium sulphide, displayed significant anti-fungal property against the pathogenic yeast *Candida albicans* (MTCC 227) at a minimum fungicidal concentration of 300 μg/ml. The antifungal property of zinc sulphide particles is attributed to the generation of reactive oxygen species due to the interaction of nanoparticles with water. Additionally, the presence of Zn and S in the zone of inhibition area and the absence of antifungal effects for large micron sized particles of ZnS suggests size induced effects leading to perturbation of fungi cell membranes resulting in growth inhibition.

Keywords: ZnS, nanoparticles, green and energy efficient synthesis, sonochemical, anti-microbial, anti-fungal, nanocrystals,

Introduction

Control of microbial growth has become increasingly difficult owing to the resistance offered by microbes against conventional anti microbial agents. The use of nanoparticles such as TiO$_2$, ZnO, Ag etc. [1-10] for anti-microbial activity has been successfully demonstrated in recent times. Nanoparticles of ZnO and silver [10-15] are developed as novel anti bacterial agents as these particles are prepared by simple and cost effective techniques such as chemical precipitation with good control over particle sizes, surface area and stoichiometry. A host of mechanisms are postulated to explain the anti bacterial effect of nanosized particles. The generation of reactive oxygen species [8,10,16-18] primarily through photo induced mechanisms is a prominent cause for anti microbial activity in nanosized particles of titania and ZnO. The effect of particle size on the viability of such microbes is also addressed and generally the anti microbial property increases with decreasing particle size [19-21]. An efflux mechanism leading to release of ions is also observed in certain cases [11,22]. Internalisation of nanoparticles below a threshold size and the presence of certain organic species like diethylene glycol in the medium are also reported to be effective in anti microbial action [23]. While majority of work has been carried out on metal oxide nanoparticles, recent works report the use of zinc sulphide nanoparticles for antibacterial action [24-25].

Bulk ZnS particles possess a band gap of 3.6 eV while nanosized particles derived through chemical precipitation techniques possess band gap values greater than 3.6 eV due to quantum confinement effect. However, doping with metallic ions like Ag, Ni, Mn etc. shifts the band gap of ZnS particles enabling them to be visible light active [26-28]. This is primarily ascribed to the presence of mid energy levels induced by the defects in the crystal. Thus

addition of Ag on microwave synthesised ZnS particles, lead to an increase in the photocatalytic activity under indoor light [26]. High surface area nanoporous ZnS nanoparticles in the form of uniform spheres displayed effective photocatalysis in the degradation of eosin B under visible light conditions [29].Ni doped nanostructured ZnS photocatalysts prepared by ultrasonic spray pyrolysis were successfully employed for hydrogen production under visible light irradiation [27].Studies on photocatalysis of ZnS particles have prompted researchers to explore the antimicrobial activity of such particles through photoactive mechanisms. The relative ease with which ZnS particles are prepared makes them a commercially viable candidate material for antimicrobial applications [24-25].

Pillai and co-workers recently demonstrated the anti-bacterial activity of nanocrystalline ZnS, through the degradation of *Staphylococcus aureus* and *Escherichia coli* both in the light and dark conditions [25]. In an earlier report, ZnS nano spheres prepared by a facile one pot synthesis involving the surfactant dodecyldimethyl ammonium bromide exhibited high antibacterial activity and negligible mammalian cell toxicity [24]. However, to the best of our knowledge, the anti-fungal properties of nano ZnS have not been explored yet. In this current investigation, we report the use of ZnS nanoparticles, synthesised by an ultrasonic assisted precipitation technique, for anti-fungal activity against the fungus *Candida albicans*.

2. Experimental

2.1.   *Preparation of ZnS Nanoparticles*

ZnS particles were synthesised by the chemical reaction of zinc chloride with sodium sulfide in solutions. In a typical synthesis, 125 ml of 0.5 M aqueous solution of zinc chloride was subjected to ultrasonic irradiation using a probe sonicator (Vibronics, Mumbai, India). During sonication, 125 ml of 0.5 M sodium sulphide solution was added drop wise and the sonication was continued for 45 minutes when a whitish yellow thick precipitate of ZnS was

obtained. The product was washed with excess amount of water to remove any unreacted species and dried further in an oven at 70^0 C.

For comparison experiments, commercially available ZnS particles (Aldrich, Bangalore, India) were used

2.2. *Characterisation*

The ZnS obtained from sonochemical precipitation was characterised by X-ray diffraction using XRD (PW1710 Phillips, The Netherlands) in the 2θ range of 10-80^0 using a Cu Kα radiation source. Scherrer equation (Equation 1) was employed for the determination of crystallite sizes of the ZnS samples.

$$\emptyset = \frac{K \lambda}{\beta Cos\theta}$$

Where φ is the crystallite size, λ is the wavelength of X-ray, K is the shape factor, and β the full line width at the half-maximum height of the major intensity peak. Luminescence spectrum was taken using a spectrofluorometer (Cary Eclipse, Varian, Netherlands). Powder morphology of synthesized particles was imaged under transmission electron microscope (Tecnai G^2, FEI, The Netherlands operated at 300 kV). Particle size measurements were performed by photo-correlation spectroscopy of dilute suspensions of ZnS particles .The BET surface area studies were carried out using a BET surface area analyser (Gemini 2375, Micromeritics, USA) after degassing the samples at 200^0 C for 2 hours. Observation of fungi before and after exposure to ZnS were performed by scanning electron microscope (Carl Zeiss, Germany).

2.3. *Anti-fungal studies*

2.3.1. Disc diffusion method

Agar disc diffusion method for antifungal tests was carried out using potato dextrose agar [30]. The inoculum was prepared using 24 h plate cultures of test fungi *Candida albicans* (MTCC 227). The colonies were suspended in 0.85% saline and the turbidity was compared with the 0.5 McFarland standards, to produce a suspension of 1×10^6 CFU/ml. The suspension was loaded on a sterile cotton swab that was rotated several times and pressed firmly against the inside wall of the tube to remove excess inoculum from the swab. The dried surface of a potato dextrose agar plate was inoculated by streaking the swab over the entire sterile agar surface. The discs of ZnS prepared from both the synthesized nanoparticles (n-ZnS) and commercially available micron sized (m-ZnS) particles (0.3g, 11 mm diameter) were placed on the top of the inoculated plates and were incubated at 30^0C for 48 h. The antifungal activity was evaluated by measuring the zone of growth inhibition surrounding the discs. Larger the diameter of zone of inhibition, greater is the antimicrobial activity.

2.3.2. *Effect of ZnS concentration on C. albicans*

Cultures of *C. albicans* grown on potato dextrose agar broth for 24 h were used for the quantitative antifungal studies by optical density method (OD) at 600 nm. Viability and growth curve of *C. albicans* were measured by adding different amounts of ZnS nanoparticles in to the culture (3×10^5 CFU/ml) and subsequently measuring the OD at different time intervals. Control experiments were performed on cultures without n-ZnS particles

2.3.3 *Determination of minimum fungicidal concentration of ZnS on C. albicans growth*

The minimum fungicidal concentration (MFC) of ZnS nanoparticles on *C. albicans* were resolved by adding different concentrations of ZnS nanoparticles into the *C. albicans* culture and measuring the OD after 18 h.

### 2.3.4. *Role of reactive oxygen species in antifungal activity*

The role of reactive oxygen species (ROS) in antifungal activity is evaluated with the aid of histidine, a known ROS scavenger material. In this *C. albicans* culture containing a specific

amount of ZnS nanoparticles (300 µg/ml) was treated with different concentrations of histidine and the change in OD was monitored at different time intervals. Control experiments were performed as mentioned above.

3. Results

3.1 X-ray diffraction

Figure 1 presents the x-ray diffraction patterns of sonochemically synthesised ZnS in comparison with that of commercial ZnS. The peak positions for both the ZnS particles are at 2θ values of 28.6, 47.5 and 56.3 corresponding to the (111), (220) and (311) planes respectively confirmed the crystallisation of ZnS in cubic blende structure.
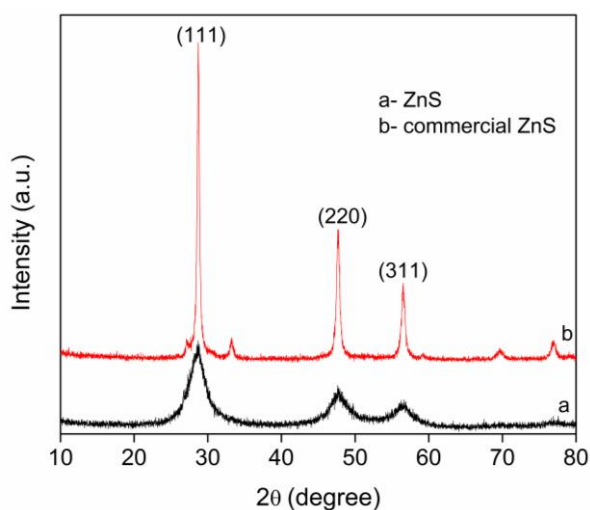

Fig. 1 XRD patterns of a) ZnS particles synthesised by sonochemical route and b) commercially obtained.

Crystallite size of 3.4 ± 1 nm was estimated from the diffraction data using the Scherer equation and calculated from the full width half maxima (FWHM) of (111) peak. The m-ZnS displayed well defined peaks characteristic of highly crystallised particles and additional peaks at 2Θ values of 70 and 78 corresponding to sphalerite phases are also seen.

3.2 Particle size distribution

The particle size distribution of n-ZnS and m-ZnS was estimated using photo correlation spectroscopy and the number average plots are presented in Fig. 2. The nano ZnS particles, in the absence of surface modifiers, are in agglomerated form and the average agglomerate size is above 100nm. The commercial ZnS particles were distinctly larger with particle sizes values larger than 2 microns.
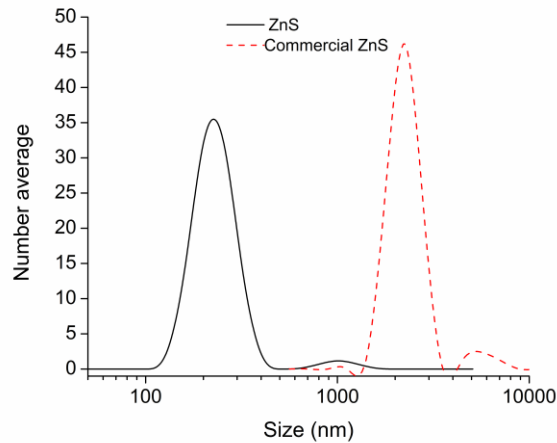
Fig. 2 Particle size distribution plots for a) ZnS particles synthesised by sonochemical route and b) commercially obtained.

3.3   *Transmission Electron Microscopy*

Fig. 3 provides the TEM images of nano ZnS particles derived from the sonochemical precipitation. The particles appear agglomerated which is a characteristic feature of surfactant free precipitation reactions in aqueous medium. Primary particles of size 4-5nm are found spherical in morphology and exhibited a narrow distribution within the aggregates.
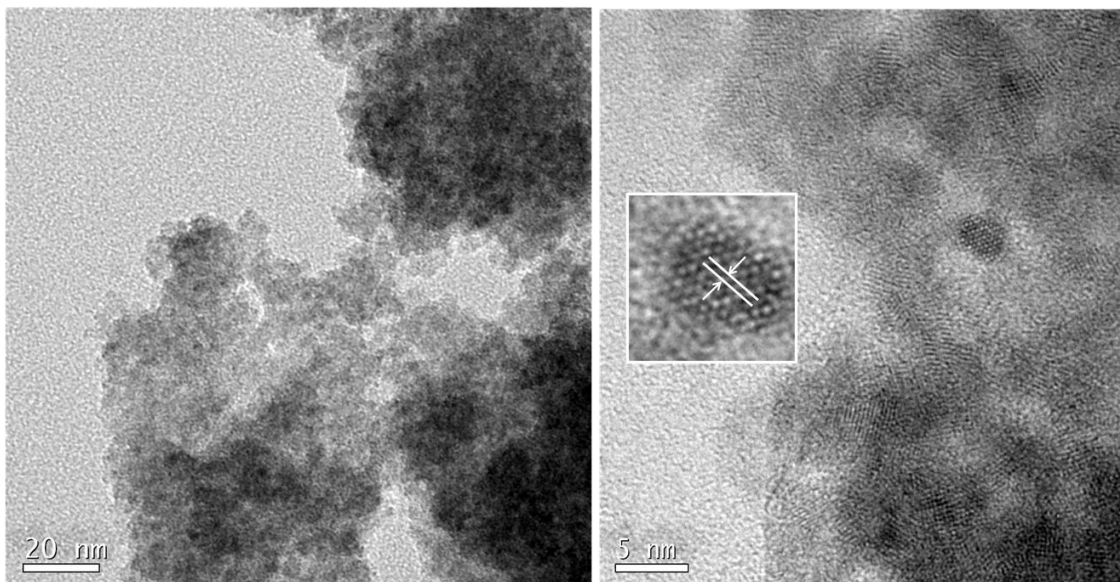
Fig. 3 TEM image of ZnO particles obtained by sonochemical precipitation and HRTEM image showing individual particles.

This particle size value is in line with the crystallite size value of 3.4 $\pm$ 1 nm measured by XRD. The HRTEM image shown in Fig 3b indicates the appearance of lattice fringes confirming the crystallinity. The distance between two fringes is calculated (inset) to be 0.3nm and is in good agreement for ZnS nanoparticles.

3.4 Disc Diffusion Test for Antifungal activity

The n-ZnS and m-ZnS particles were then subjected to anti-fungal activity (against *C. albicans*) using the disc diffusion method. Fig. 4a and 4b represent the photographs of agar plates containing ZnS discs (0.3 g, 11 mm diameter) inoculated with *C. albicans* fungi. The zone of inhibition, approximately 29.8mm in diameter, surrounding the n-ZnS disc obtained from the sonochemical precipitation clearly demonstrated the anti fungal property of nano zinc sulphide particles. In contrast, the m-ZnS disc obtained from commercial ZnS particles indicated negligible action as indicated by the absence of zone of inhibition.
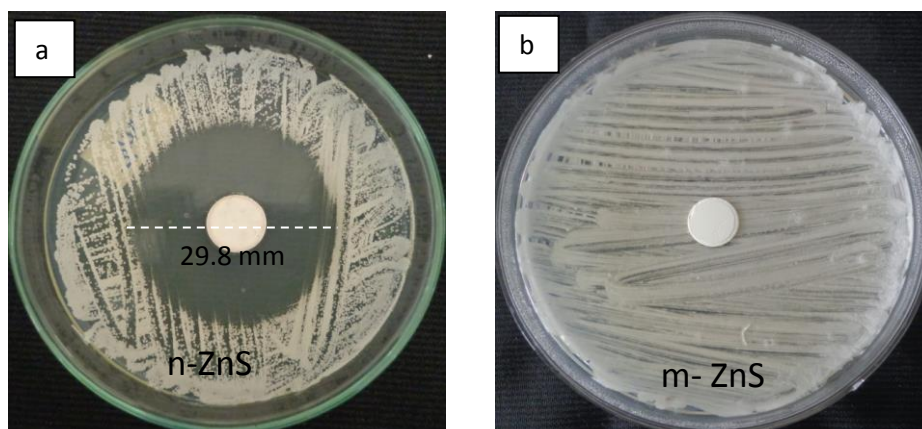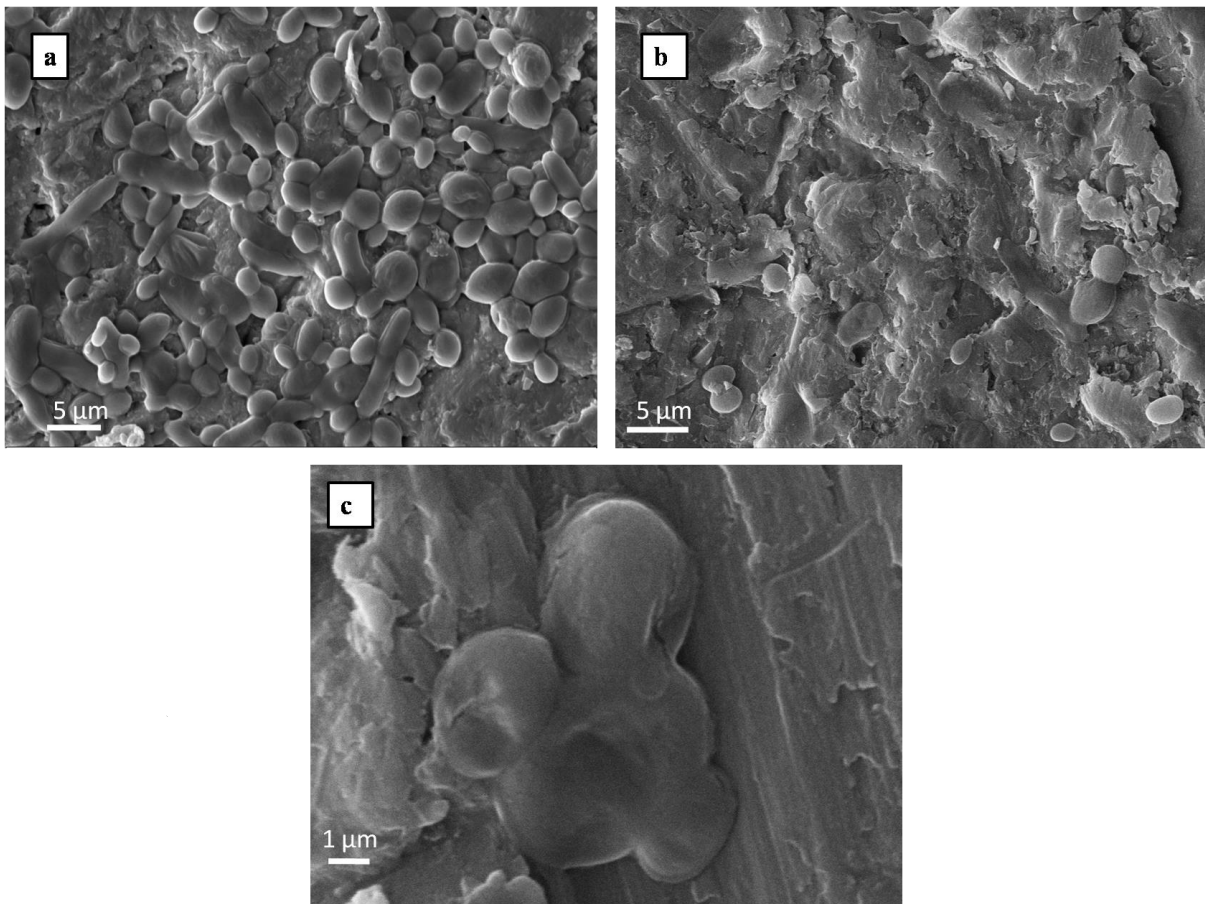
Fig. 4 Photographs of agar medium containing a) n-ZnS and b) m-ZnS after 24hours displaying the results of zone of inhibition test.

### 3.5   Cell morphology by SEM imaging

The SEM images of *C. albicans* with n-ZnS particles at 0 and 24 h durations are presented in Fig. 5(a-c). In Fig. 5a, the oval shaped unicellular fungi are seen spread over the broth at the start of the test. Elongated cells are also occasionally observed. After 24 h there is considerable decrease in the number of fungi cells observed. The magnified micrograph presented in Fig. 5c captures the decay of fungi cells.

Fig. 5 SEM micrographs of agar medium containing n-ZnS particles at a) start of the test b) after 24h c) Higher magnification image of b.

3.6   Growth Curves of C. albicans in presence of n-ZnS

The ability of n-ZnS particles to inhibit the growth of *C. albicans* was explored using different concentrations of n-ZnS particles in comparison with a control sample without ZnS. Fig. 6 represents the optical density at 600nm against time for the n- ZnS concentration ranges of 50-300 μg/ml. It is clearly evident from the growth curves that the presence of n-ZnS particles retarded the growth of *C. albicans*. The growth inhibition was strongly influenced by the n-ZnS concentration and the steep rise in the growth curve observed for the control sample is significantly reduced in the presence of n-ZnS particles. It is also observed that the logarithmic phase of growth curve is delayed and the growth rate decreased with increasing concentration of n-ZnS as has been observed in the case of ZnO nanoparticles (ZnO NP)[8]
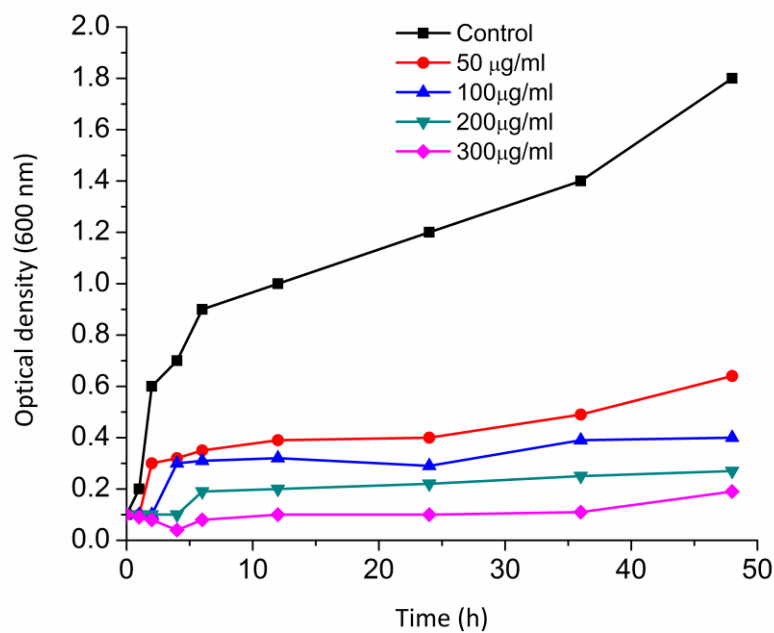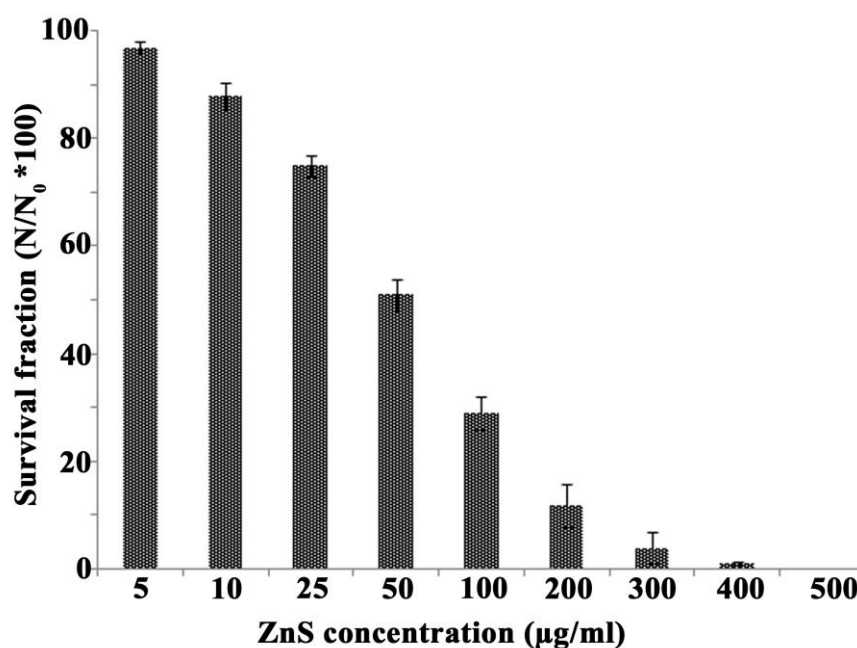

Fig. 6 Growth curves of *C. albicans* with varying concentrations of n-ZnS particles compared with that of a control sample.

3.7   *Minimum Fungicidal Concentration (MFC)*

The lowest concentration of n-ZnS particles required to affect the viability of *C. albicans* was elucidated by a measurement of Minimal Fungicidal Concentration (MFC). Different

concentrations of ZnS nanoparticles (5-500 μg/ml) were added to *C. albicans* cultures and the

survival fractions were analysed (Fig. 7). It has been found that the cell counts of *C. albicans*

decreased as the concentration of ZnS increases. A minimum of 300 μg/ml concentration of

n-ZnS was essential to realise >90% fungicidal activity

Fig. 7 Estimation of survival fractions of *C. albicans* with varying concentrations of n-ZnS

particles.

3.8   *Role of Histidine on growth curves of C.albicans*

Results shown in Fig. 4, 6 and 7 clearly indicated that the presence of ZnS nanoparticles (n-

ZnS) or pellets made out of n-ZnS inhibited the growth of *C.albicans.* The most likely

mechanism contributing to the antifungal activity by nanoparticles is the generation of

reactive oxygen species. One of the methods to validate the ROS mechanism is the use of

hydroxyl radical scavengers like histidine [8,31].   In the present study, the effect of histidine on

the fungicidal activity of n-ZnS particles was studied by analysing the optical density with

time. Growth curves of cultures containing n-ZnS particle (300 μg/ml) and varying amounts

of histidine were estimated and the data presented in Fig. 8 clearly demonstrated a concentration dependent influence of histidine on the fungicidal activity of n-ZnS. It was found that fungicidal activity was lower at higher histidine concentrations. Sample containing n-ZnS and 4mM histidine showed growth profile that more or less matched that of the control sample (without n-ZnS particles) indicating that the generated ROS is effectively scavenged by histidine. The results thus obtained revealed that the antifungal activity of n-ZnS particles is primarily related to the ROS mechanism.
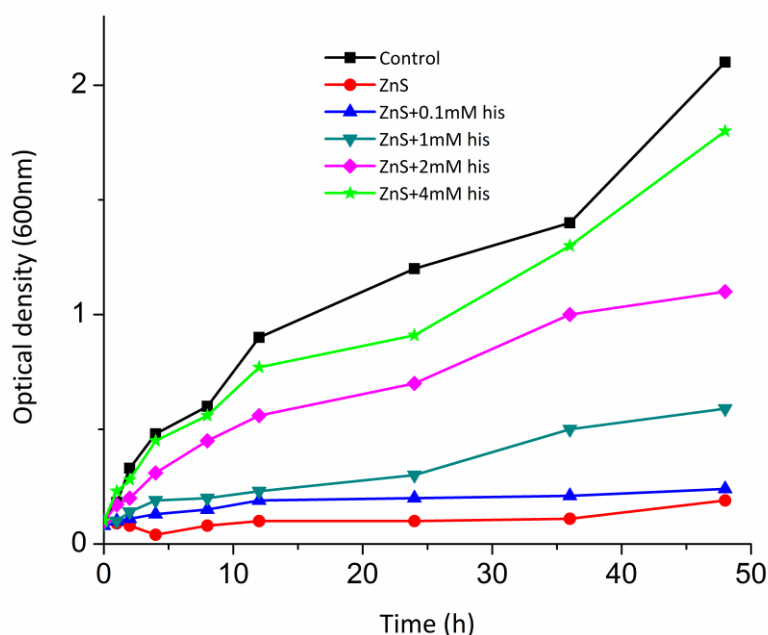
Fig. 8 Growth curves of C.albicans in n-ZnS cultures containing varied concentrations of histidine.

3.9   *Photoluminescence Spectrum*

The luminescence spectrum of ZnS nanoparticles upon excitation at 270 nm is presented in Fig. 9. The broad peak observed in the wavelength region of 340-350 nm is generally ascribed to interstitial Sulphur [32-33]. The presence of interstitial zinc is denoted by the small peak observed in the wavelength region of 392-395 nm [32-33]. The most prominent peak at

432 nm is characteristic of S vacancies in ZnS powders. The minor peak at 490 nm is associated with Zn vacancies [32-33]. The observed peaks and their related defects suggest the existence of donor levels within the band gap.
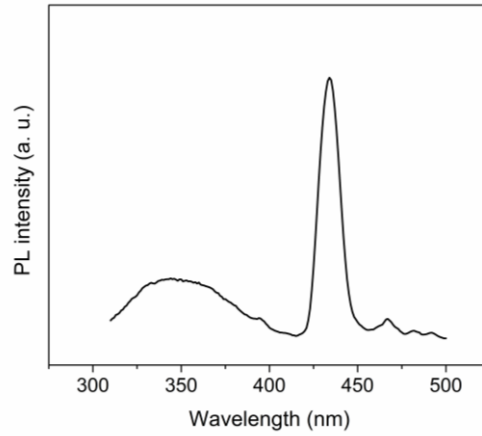
Fig. 9 Photoluminescence spectra of n-ZnS particles

3.10   Zn elemental mapping

In order to explore the possibility of mechanisms other than ROS, we have carried out elemental mapping studies on the zone of inhibition area and Fig. 10 plots the Zn/Cl ratio against the distance from the outer edge of the disc in the zone of inhibition.
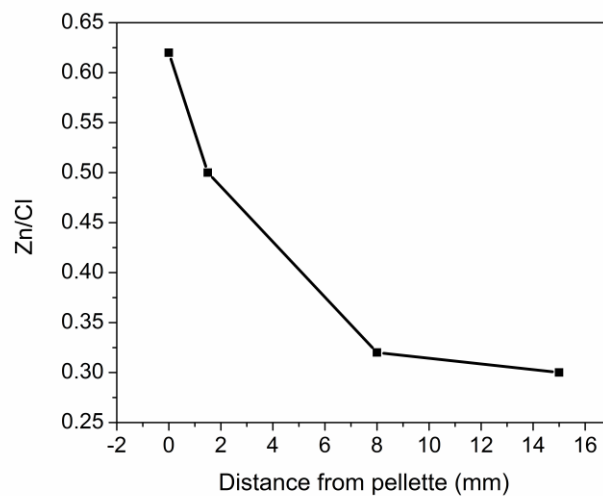
Fig. 10 Variation of zinc concentration along the diameter of zone of inhibition (Cl from brine solution was present in the reaction medium uniformly and was taken as the standard against which the decay in Zn concentration is represented)

As shown, there is a gradual decrease in the Zn concentration along the radius of the zone of inhibition. The presence of Zn along the zone of inhibition area is presumably an indication of the Zn^{2+} efflux mechanism also contributing towards the antifungal activity.

4.0   Discussion

The antimicrobial property of nanoparticles is ascribed to a combination of factors that include generation of ROS and efflux mechanisms leading to the release of constituent ions [1,8,11-12,22]. The disruption of the cell membrane activity by the direct contact between the nanoparticles and cell membrane is also reported to be responsible for antifungal activity of ZnO nanoparticles [17,34]. The binding of nanoparticles to the microbe cell membrane by direct or electrostatic forces affect the permeability of membranes and induces an oxidative stress preventing cell growth[17,35-36]. It was previously shown that smaller the particle size, the greater will be the antimicrobial activity[19-20,37-39]. In the present study, the n-ZnS particles obtained by the sonochemical precipitation displayed remarkable antifungal action at a minimum fungicidal concentration of 300 μg/ml. The inhibition of antifungal activity on addition of 4mM histidine suggested the generation of ROS to be the most likely mechanism. n-ZnS with its intrinsic defects (clear from photoluminescence spectra) produced electron-hole pairs. The holes reacted with water producing H^+ and OH^- ions and the electrons converted dissolved oxygen molecules to superoxide radical anions. The superoxide radical anions thus obtained reacted with H^+ producing $HO_2^{\cdot}$ radicals which are in turn converted to hydrogen peroxide anions (HO_2^-). Hydrogen peroxide is then obtained by the reaction of

these anions with hydrogen ions. The peroxide can penetrate the fungi cell membrane and disrupt them due to oxidative stress[18,40]. The generation of hydrogen peroxide thus forms the basis of antimicrobial activity in such nanoparticles. In the present study, the antifungal tests were all performed without light irradiation and therefore the genesis of hydrogen peroxide may not be ascribed to a photo induced mechanism. In a very recent article[41], three kinds of ZnO namely tetrapod like ZnO whiskers, nanosized ZnO particles and micron sized ZnO particles were tested for antimicrobial activity against E.coli and the authors invoked a mechanism based on the oxygen vacancies in the surface layer of ZnO. The particle size and surface area of the three types of ZnO samples were shown to be less influential on the generation of H_2O_2. In the case of n-ZnS, the presence of S vacancies, substantiated by PL measurements, is the most obvious source of band transitions leading to the generation of H_2O_2. The observance of fungicidal activity without light irradiation is thus presumed to be due to availability of sulphur vacancies providing donor levels within the band gap.

The diffusion of Zn^{2+} in the agar medium and its activity with the cell membranes of the fungi should directly influence the size of zone of inhibition. It should be noted that the n-ZnS nanoparticles displayed a zone of inhibition of ~ 30 mm diameter. Elemental mapping studies revealed the leaching of n-ZnS particles in the inhibition zone. The concentration of Zn in the zone of inhibition was highest close to the n-ZnS disc and it gradually decreased along the radius of the zone of inhibition. This suggested the likelihood of an efflux mechanism also where Zn^{2+} ions can cross the fungi cell membrane causing irreversible damage effecting cell death.

The most widely investigated nano particle system for antifungal activity is ZnO. The minimum fungicidal concentration reported for ZnO varies in the range of 30 to 200 μg/ml

depending on the method of synthesis. In the present study the MFC of n-ZnS particles was observed to be around 300 μg/ml. The difference in MFC of ZnO and ZnS can presumably be due to the availability of dissolved oxygen species, in ZnO containing medium, arising out of the oxygen related defects like oxygen vacancies [11,41-42]. However, due to the large difference in solubility of ZnO and ZnS in water (nano ZnO particles are shown to be soluble up to 7-7.5mg/L while ZnS possesses negligible solubility) the outdoor applications of ZnS based antifungal agents can be of longer durability.

Conclusions

This work, to the best of our knowledge, constitutes the first study of antifungal property of ZnS nanoparticles against the increasingly drug resistant fungus *Candida Albicans*. The sonochemical synthetic route produced n-ZnS particles with S vacancies that lead to the generation of hydrogen peroxide in aqueous suspensions. The generation of ROS as the dominating mechanism is confirmed by the observation that the fungicidal activity of n-ZnS particles is inhibited by 4mM addition of histidine, a scavenger of hydroxyl radical and singlet oxygen. Additionally, elemental mapping studies carried out along the radius of the zone of inhibition area revealed the presence of Zn in decreasing concentrations. This efflux mechanism releasing Zn^{2+} ions also contribute towards disruption of fungi cell membrane inducing irreversible damage and cell death. Zinc sulphide nanoparticles thus emerge as a potential antifungal agent that can be used to eliminate fungi related infections.

References

[1]   N. Perkas, A. Lipovsky, G. Amirian, Y. Nitzan and A. Gedanken, *Journal of Materials Chemistry B*, 2013, 1**,** 5309.

[2]   K. Page, R. G. Palgrave, I. P. Parkin, M. Wilson, S. L. P. Savin and A. V. Chadwick, *Journal of Materials Chemistry*, 2007, 17**,** 95.

[3]   C. W. Dunnill, Z. A. Aiken, A. Kafizas, J. Pratten, M. Wilson, D. J. Morgan and I. P. Parkin, *Journal of Materials Chemistry*, 2009, 19**,** 8747.

[4]   C. W. Dunnill, Z. Ansari, A. Kafizas, S. Perni, D. J. Morgan, M. Wilson and I. P. Parkin, *Journal of Materials Chemistry*, 2011, 21**,** 11854.

[5]   H. Bai, Z. Liu and D. D. Sun, *Physical Chemistry Chemical Physics*, 2011, 13**,** 6205.

[6]   S. Ghosh, V. S. Goudar, K. G. Padmalekha, S. V. Bhat, S. S. Indi and H. N. Vasan, *RSC Advances*, 2012, 2**,** 930.

[7]   T. Gordon, M. Kopel, J. Grinblat, E. Banin and S. Margel, *Journal of Materials Chemistry*, 2012, 22**,** 3614.

[8]   A. Lipovsky, Y. Nitzan, A. Gedanken and R. Lubart, *Nanotechnology*, 2011, 22**,**

[9]   N. E. A. El-Gamel, *Dalton Transactions*, 2013, 42**,** 9884.

[10]   I. Perelshtein, E. Ruderman, N. Perkas, T. Tzanov, J. Beddow, E. Joyce, T. J. Mason, M. Blanes, K. Molla, A. Patlolla, A. I. Frenkel, A. Gedanken, *Journal of Materials Chemistry B*, 2013, 1**,** 1968.

[11]   A. S. Haja Hameed, C. Karthikeyan, S. Sasikumar, V. Senthil Kumar, S. Kumaresan and G. Ravi, *Journal of Materials Chemistry B*, 2013,

[12]   Y. Wang, F. Huang, D. Pan, B. Li, D. Chen, W. Lin, X. Chen, R. Li and Z. Lin, *Chemical Communications*, 2009, 6783.

[13]   S. Agnihotri, S. Mukherji and S. Mukherji, *Nanoscale*, 2013, 5**,** 7328.

[14]   M. Nocchetti, A. Donnadio, V. Ambrogi, P. Andreani, M. Bastianini, D. Pietrella and L. Latterini, *Journal of Materials Chemistry B*, 2013, 1**,** 2383.

[15]   M. A. Gondal, A. J. Alzahrani, M. A. Randhawa and M. N. Siddiqui, *Journal of Environmental Science and Health Part a-Toxic/Hazardous Substances & Environmental Engineering*, 2012, 47**,** 1413.

[16]   G.-X. Tong, F.-F. Du, Y. Liang, Q. Hu, R.-N. Wu, J.-G. Guan and X. Hu, *Journal of Materials Chemistry B*, 2013, 1**,** 454.

[17]   P. K. Stoimenov, R. L. Klinger, G. L. Marchin and K. J. Klabunde, *Langmuir*, 2002, 18**,** 6679.

[18]   G. Applerot, A. Lipovsky, R. Dror, N. Perkas, Y. Nitzan, R. Lubart and A. Gedanken, *Advanced Functional Materials*, 2009, 19**,** 842.

[19]   J. Sawai, H. Igarashi, A. Hashimoto, T. Kokugan and M. Shimizu, *Journal of Chemical Engineering of Japan*, 1996, 29**,** 251.

[20]   O. Yamamoto, *International Journal of Inorganic Materials*, 2001, 3**,** 643.

[21]   S. Nair, A. Sasidharan, V. V. Divya Rani, D. Menon, S. Nair, K. Manzoor and S. Raina, *Journal of materials science. Materials in medicine*, 2009, 20 Suppl 1**,** S235.

[22]   Z. H. Yang and C. S. Xie, *Colloids and Surfaces B-Biointerfaces*, 2006, 47**,** 140.

[23]   R. Brayner, R. Ferrari-Iliou, N. Brivois, S. Djediat, M. F. Benedetti and F. Fievet, *Nano Letters*, 2006, 6**,** 866.

[24]   G. Li, J. Zhai, D. Li, X. Fang, H. Jiang, Q. Dong and E. Wang, *Journal of Materials Chemistry*, 2010, 20**,** 9215.

[25]   D. W. Synnott, M. K. Seery, S. J. Hinder, G. Michlits and S. C. Pillai, *Applied Catalysis B-Environmental*, 2013, 130**,** 106.

[26]   D. W. Synnott, M. K. Seery, S. J. Hinder, J. Colreavy and S. C. Pillai, *Nanotechnology*, 2013, 24**,**

[27]   J. H. Bang, R. J. Helmich and K. S. Suslick, *Advanced Materials*, 2008, 20**,** 2599.

[28]   H. R. Pouretedal, A. Norozi, M. H. Keshavarz and A. Semnani, *Journal of Hazardous Materials*, 2009, 162**,** 674.

[29]   J. S. Hu, L. L. Ren, Y. G. Guo, H. P. Liang, A. M. Cao, L. J. Wan and C. L. Bai, *Angewandte Chemie International Edition*, 2005, 44, **1269**.

[30]   S. Ghasemi, S. Abbasi, S. Bahraminejad and B. Harighi, *Australasian Plant Pathology*, 2012, 41, **331**.

[31]   M. Shoeb, R. S. Braj, A. K. Javed, K. Wasi, N. S. Brahma, B. S. Harikesh and H. N. Alim, *Advances in Natural Sciences: Nanoscience and Nanotechnology*, 2013, 4, 035015.

[32]   M. V. Limaye, S. Gokhale, S. A. Acharya and S. K. Kulkarni, *Nanotechnology*, 2008, 19,

[33]   A. V. Murugan, O. Y. Heng, V. Ravi, A. K. Viswanath and V. Saaminathan, *Journal of Materials Science*, 2006, 41, **1459**.

[34]   R. Brayner, R. Ferrari-Iliou, N. Brivois, S. Djediat, M. F. Benedetti and F. Fiévet, *Nano Letters*, 2006, 6, **866**.

[35]   Y. Xie, Y. He, P. L. Irwin, T. Jin and X. Shi, *Applied and Environmental Microbiology*, 2011, 77, **2325**.

[36]   L. Zhang, Y. Jiang, Y. Ding, M. Povey and D. York, *Journal of Nanoparticle Research*, 2007, 9, **479**.

[37]   J. Sawai and T. Yoshikawa, *Journal of Applied Microbiology*, 2004, 96, **803**.

[38]   O. Yamamoto, M. Hotta, J. Sawai, T. Sasamoto and H. Kojima, *Journal of the Ceramic Society of Japan*, 1998, 106, **1007**.

[39]   S. Makhluf, R. Dror, Y. Nitzan, Y. Abramovich, R. Jelinek and A. Gedanken, *Advanced Functional Materials*, 2005, 15, **1708**.

[40]   M. Fang, J. H. Chen, X. L. Xu, P. H. Yang and H. F. Hildebrand, *International Journal of Antimicrobial Agents*, 2006, 27, **513**.

[41]   X. Xu, D. Chen, Z. Yi, M. Jiang, L. Wang, Z. Zhou, X. Fan, Y. Wang and D. Hui, *Langmuir*, 2013, 29, **5573**.

[42]   J. Becker, K. R. Raghupathi, J. St. Pierre, D. Zhao and R. T. Koodali, *The Journal of Physical Chemistry C*, 2011, 115, **13844**.